

Bandwidth expansion and pulse shape optimized for 10 PW laser design via spectral shaping

Da-Wei Li(李大为), Tao Wang(王韬), Xiao-Lei Yin(尹晓蕾), Li Wang(王利), Jia-Mei Li(李佳美),Hui Yu(余惠), Yong Cui(崔勇), Tian-Xiong Zhang(张天雄), Xing-Qiang Lu(卢兴强), and Guang Xu(徐光)

Citation: Chin. Phys. B, 2022, 31 (**9**): 094210. DOI: 10.1088/1674-1056/ac6018
Journal homepage: http://cpb.iphy.ac.cn; http://iopscience.iop.org/cpb

What follows is a list of articles you may be interested in

Switchable instantaneous frequency measurement by optical power monitoring based on DP-QPSK modulator

Yu-Lin Zhu(朱昱琳), Bei-Lei Wu(武蓓蕾), Jing Li(李晶), Mu-Guang Wang(王目光), Shi-Ying Xiao(肖世莹), and Feng-Ping Yan(延凤平)
Chin. Phys. B, 2022, 31 (**4**): 044202. DOI: 10.1088/1674-1056/ac40ff

Color-image encryption scheme based on channel fusion and spherical diffraction

Jun Wang(王君), Yuan-Xi Zhang(张沅熙), Fan Wang(王凡), Ren-Jie Ni(倪仁杰), and Yu-Heng Hu(胡玉衡)
Chin. Phys. B, 2022, 31 (**3**): 034205. DOI: 10.1088/1674-1056/ac1b87

Design of an augmented reality display based on polarization grating

Renjie Xia(夏人杰), Changshun Wang(王长顺), Yujia Pan(潘雨佳), Tianyu Chen(陈天宇), Ziyao Lyu(吕子瑶), Lili Sun(孙丽丽)
Chin. Phys. B, 2019, 28 (**7**): 074201. DOI: 10.1088/1674-1056/28/7/074201

Macadam's theory in RGB laser display

Guan Wang(王贯), Yuhua Yang(杨雨桦), Tianhao Dong(董天浩), Chun Gu(顾春), Lixin Xu(许立新), Zhongcan Ouyang(欧阳钟灿), Zuyan Xu(许祖彦)
Chin. Phys. B, 2019, 28 (**6**): 064209. DOI: 10.1088/1674-1056/28/6/064209

Optical encryption of multiple three-dimensional objects based on multiple interferences and single-pixel digital holography

Ying Wang(王莹), Qi Liu(刘琦), Jun Wang(王君), Qiong-Hua Wang(王琼华)
Chin. Phys. B, 2018, 27 (**3**): 034202. DOI: 10.1088/1674-1056/27/3/034202

Bandwidth expansion and pulse shape optimized for 10 PW laser design via spectral shaping

Da-Wei Li(李大为)[1,4], Tao Wang(王韬)[2,†], Xiao-Lei Yin(尹晓蕾)[3], Li Wang(王利)[1], Jia-Mei Li(李佳美)[1,4], Hui Yu(余惠)[1,4], Yong Cui(崔勇)[2], Tian-Xiong Zhang(张天雄)[2], Xing-Qiang Lu(卢兴强)[1,‡], and Guang Xu(徐光)[1]

[1] *Key Laboratory of High Power Laser and Physics, Shanghai Institute of Optics and Fine Mechanics, Chinese Academy of Sciences, Shanghai* 201800, *China*
[2] *Shanghai Institute of Laser Plasma, Chinese Academy of Engineering Physics, Shanghai* 201800, *China*
[3] *Changzhou Institute of Technology, School of Sciences, Changzhou* 213032, *China*
[4] *Center of Materials Science and Optoelectronics Engineering, University of Chinese Academy of Sciences, Beijing* 100049, *China*

(Received 30 December 2021; revised manuscript received 10 March 2022; accepted manuscript online 23 March 2022)

We demonstrated a scheme of bandwidth expansion and pulse shape optimized to afford 10 PW laser design via spectral shaping, which uses the existing Nd:glass amplifier chain of the SG PW laser. Compared to the amplified pulse with a gain-narrowing effect, the required parameters of injected pulse energy, spectral bandwidth, and shape are analyzed, together with their influence on the system B-integral, energy output capability, and temporal intensity contrast. A bandwidth expansion to 7 nm by using $LiNbO_3$ birefringent spectral shaping resulted in an output energy of 2 kJ in a proof-of-principle experiment. The results are consistent with the theoretical prediction which suggests that the amplifier chain of SG PW laser is capable of achieving 6 kJ at the bandwidth of 7 nm and the B-integral $< \pi$. This will support a 10 PW laser with a compressed pulse energy of 4.8 kJ (efficiency = 80%) at 480 fs.

Keywords: SG PW laser, bandwidth expansion, B-integral, spectral shaping

PACS: 42.40.My, 42.25.Lc, 42.15.Eq **DOI:** 10.1088/1674-1056/ac6018

1. Introduction

Since the advent of chirped pulse amplification technology, alongside several to hundreds of nanosecond laser beams,[1–5] the kilojoule-level and picosecond petawatt (PW, 10^{15} W) lasers, which are mainly based on the same amplified chain, play important roles in the experiments concerning inertial confinement fusion (ICF)[6–8] and high-energy density sciences.[9–12] However, compared to the energy of the 17 kJ level for nanosecond pulses, the amplified energy of the kilojoule-level PW laser pulse is mainly limited by the system B-integral, which should be designed to be not larger than two to guarantee the compressed pulse duration and temporal contrast.[13] In addition, the gain-narrowing effect reduces the spectrum bandwidth to 3 nm, while also shortening the pulse duration of the chirped pulse; this restricts the energy of the amplified pulse because of the limited damage threshold of optical elements. Furthermore, the bandwidth limits the compressed pulse duration, which cannot be less than 470 fs.[14–17] Therefore, to improve the existing PW laser to achieve 5 PW–10 PW peak power with multi-kJ energy and duration of hundred femtoseconds, bandwidth expansion, and pulse shape optimized by compensating the gain-narrowing via spectral shaping is a better alternative.

There are many spectral shaping methods for bandwidth expansions. However, acoustic optic programmable dispersion filters (AOPDFs)[18] and spatial light modulators (SLMs)[19] are only employed for low energies because of their limited damage threshold. The spectral shapes controlled by the time shape of the pump laser in optical parametric chirped-pulse amplification (OPCPA)[20] and spectral filter mirror[21] are mainly used for the wider spectral bandwidth with pulse durations of 30 fs–150 fs. Additionally, these demand complicated design, expensive pump lasers, and difficult to fabricate filters, which are not suitable for the bandwidth of several nanometers of the picosecond PW lasers. Birefringent filters[22] can be used for bandwidth broadening in a regenerative amplifier with the Joule level[23] at 1054 nm, and have been predicted to improve energy by minimizing the risk of damage to mirrors.[24] Moreover, the bandwidth is extended to 15 nm with a compressed pulse duration of 150 fs using mixed glass, the energy achieves 150 J in the Texas PW laser system,[25] and larger energy is designed to 1500 J with 150 fs for ELI beamlines.[20] Compared to other picosecond PW lasers, Texas and ELI use different seed, stretcher, and amplifier modules. To the best of our knowledge, this is the first simulated design and experimental demonstration of spectral shaping using $LiNbO_3$ birefringent plate for bandwidth expansion of 7 nm with the energy of 2 kJ based on an existing picosecond PW laser.

In this study, a theoretical model for a round trip chirped pulse amplification is described. The bandwidth expansion for the SG PW laser and the corresponding system B-integral

†Corresponding author. E-mail: twang@siom.ac.cn
‡Corresponding author. E-mail: xingqianglu@siom.ac.cn

© 2022 Chinese Physical Society and IOP Publishing Ltd

are discussed, together with the output spectrum with gain-narrowing, and the required spectral shape parameters for different output bandwidths are covered. The system B-integral and depletion population inversion of the final amplifier is compared and the criterion of the B-integral for a bandwidth expansion of 7 nm is given. Furthermore, a demonstration experiment for bandwidth expansion of 7 nm with the energy of 2 kJ, which uses spectral shaping based on the $LiNbO_3$ birefringent plate and installed after OPCPA. The results suggest that the existing Nd:glass amplifier chain of SG PW laser can afford even 10 PW (4.8 kJ, 480 fs) output, which will be beneficial for the performance improvement of single PW beams and the coherent beam combination of multi-PW beams[26] in the future.

2. Theoretical model

As shown in Fig. 1, the SG PW laser system consists of five blocks.[27] (i) The seed, which is a commercial SESAM mode-locked Nd:glass oscillator (Time-Bandwidth, GLX200), achieves 250 fs pulse duration with full width at half maximum (FWHM) of 6.5 nm at 1054 nm. (ii) The stretcher, which uses the Offner structure to offer 2nd dispersion, which achieves a pulse duration of 3.3 ns. (iii) The OPCPA amplifier block, which can produce pulse energy of 60 mJ, a spectral bandwidth of 10 nm (FWHM), a pulse duration of 5 ns (5th super-Gaussian shape) at 1 Hz. (iv) The rod and disk amplifiers, which include rod (two ϕ40 mm and two ϕ70 mm rod modules) and disk amplifiers (two ϕ100 mm, three ϕ200 mm and three ϕ350 mm disk modules), and use N_{31} type Nd:glass, can amplify the chirped pulse from several millijoules to 2 kJ with 3 nm (FWHM) with B-integral of 1.72. (v) The compressor and focus, which include four 1740 lines/mm, 1 m $\times$ 0.35 m large gratings, 0.8 m off-axis parabolic mirror, vacuum system, and diagnostic equipment.

The cumulative B-integral in CPA plays an important role in determining the shape of the compressed pulses, which introduces a background pedestal and makes pulse duration wider. According to the thumb rule that the cumulative B-integral should be ≤ 2,[13] the pulse duration will be shorter than two times FTL and keep a better contrast.[27] The SG PW laser can output 2 kJ with a bandwidth of 3 nm, which is mainly limited by the designed B-integral value of 1.72[27] and the damage threshold of the mirrors. In the scheme of bandwidth expansion and pulse shape optimized in this study, a spectral shaping device based on a $LiNbO_3$ birefringent plate is placed behind the OPCPA block. After gain-narrowing compensation, the output spectral bandwidth of the CPA can be broadened, and the system B-integral and the power density on mirrors can be decreased simultaneously; therefore, the output energy can be improved compared to existing the gain-narrowing effect. Nevertheless, the spectral shape parameters required for bandwidth expansion need to be analyzed.

The propagation of light pulses in the CPA progress can be expressed as follows:[13]

$$\frac{\partial E_0(z,t)}{\partial z} = -\mathrm{i}\frac{\omega_0}{2\varepsilon c}P_0(z,t) + \mathrm{i}\frac{\beta''}{2}\frac{\partial^2 E_0(z,t)}{\partial^2 t} - \mathrm{i}\frac{\beta_2}{2}|E_0(z,t)|^2 E_0(z,t), \tag{1}$$

$$\frac{\partial P_0(z,t)}{\partial t} = -\frac{\Delta\omega_\mathrm{a}}{2}\left[1+\mathrm{i}\frac{2(\omega_0-\omega_\mathrm{a})}{\Delta\omega_\mathrm{a}}\right]P_0(z,t) + \mathrm{i}\frac{K}{2\omega_0}N(z,t)E_0(z,t), \tag{2}$$

$$\frac{\partial N(z,t)}{\partial t} = -\frac{2^*}{\hbar\omega_\mathrm{a}}\sigma_0(\lambda)N(z,t)I(z,t), \tag{3}$$

where $E(z,t)$, $P_0(z,t)$, and $N(z,t)$ are the electric field, polarization intensity, and population inversion, respectively, and z and t are the distance and time variation, respectively. ω_0 and ω_a are the carrier frequency and line center frequency, respectively. ε and c are the dielectric constant and light speed in a vacuum. β'' is the group velocity dispersion of the laser in the gain medium; $\beta_2 = 2\pi n_2/\lambda$; n_2 is the nonlinear refractive index of the transmission medium, and λ is the laser wavelength in vacuum. $\Delta\omega_\mathrm{a}$ is the full atomic linewidth; $K = \varepsilon c\sigma\Delta\omega_\mathrm{a}$; σ_0 is relevant to the stimulated emission cross-section (SECS), and $\hbar$ is the Planck constant. In this study, we do not consider the influence of the spatial distribution of the beam on broadband laser amplification, but only consider the one-dimensional case in the frequency and time domain.

Here, the electric field intensity can be described as

$$E_0(0,t) = E_0\exp\left[-\frac{1}{2}\left(\frac{t}{\tau}\right)^{2n}\right]\exp\left[-\mathrm{i}C\frac{1}{2}\left(\frac{t}{\tau}\right)^2\right], \tag{4}$$

where E_0 is the peak intensity of the initial pulse electric field; n is the Gaussian pulse order ($n = 1$ is for Gauss, and $n > 1$ is for super-Gauss); τ is the pulse duration, and C is the chirp coefficient of the broadband laser, which is generated by the stretcher and compensated by the compressor.

Equations (1)–(4) can be simulated using the split-step Fourier and Runge–Kutta methods. The inverse problem of a laser amplifier can be solved using the same methods.[28,29]

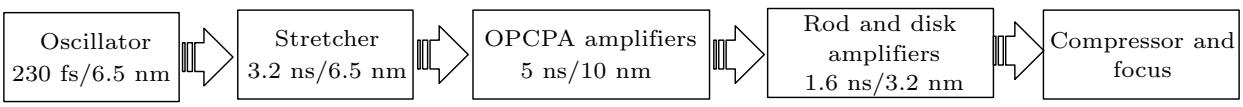


Fig. 1. Block diagram of the existing SG PW laser system.

Equation (5) shows how the B-integral, an important parameter is defined, which evaluates self-phase modulation and influences the compressed pulse duration and time fidelity,

$$B(t) = \frac{2\pi}{\lambda_0} \int_0^L n_2(z) I(z,t)\, \mathrm{d}z, \tag{5}$$

where λ_0 is the center wavelength, and L is the length of the medium. The B-integral varies with time; in this study, only the maximum B in the time domain was considered. When a birefringent plate[22,30] is used for spectral shaping, as shown in Fig. 2. The free spectral range of the plate is proportional to $1/(|\Delta n| d)$,[31] where $|\Delta n| = |n_e - n_o|$ and d is the thickness. Compared to commonly used quartz crystals with $|\Delta n| = 0.0087$ at 1053 nm, the $|\Delta n|$ of $LiNbO_3$ is 0.076, which results in the thickness of $LiNbO_3$ being nearly one-ninth to quartz, and can effectively reduce the effect of beam displacement in the experiment. Therefore, the $LiNbO_3$ birefringent plate was used here and set between two polarizers, tilted by θ (relative to the incident surface), and rotated by ϕ (relative to the optical axis). The shaped pulse energy can be controlled by a half-wave plate together with P1 to meet the injected demand. The damage threshold of $LiNbO_3$ after the coating is > 3 J/cm^2 with a maximum diameter of 76 mm, can afford high energy spectrum shaping compared to using the AOPDF and SLM.

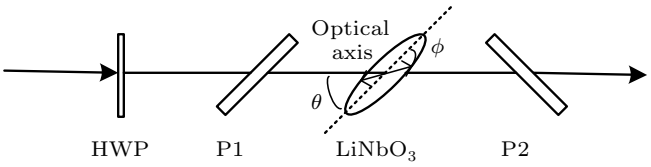


Fig. 2. Scheme of the spectral shaping based on a $LiNbO_3$ birefringent plate. P1, P2: polarizers; HWP: half-wave plate.

The electric field can be described by Eq. (6), and the intensity I_{TM} can be expressed by Eq. (7);

$$E_{TM} = \left[n_o^2 - \cos^2\phi\cos^2\theta\right]^{-1} \times \left[\exp(\mathrm{i}\delta_e) n_o^2 \sin^2\phi + \exp(\mathrm{i}\delta_o)\left(n_o^2 - \cos^2\theta\right)\cos^2\phi\right], \tag{6}$$

$$I_{TM} = E_{TM} E_{TM}^*, \tag{7}$$

where n_o is the refractive index of the ordinary polarization in the birefringent plate; δ_o and δ_e denote the optical paths of the ordinary and extraordinary transmissions in the plate. ω and ω are the laser frequency and center frequency.

3. Bandwidth expansion and pulse shape optimization

3.1. Bandwidth expansion design with gain-narrowing compensation

The gain factor, SECS spectrum of Nd:glass, and the input spectral shape constrict the bandwidth expansion of the SG PW laser. To amplify the pulse energy from the millijoule to the kilojoule level and take into account the propagation, the total gain factor is approximately 10^7. The SECS spectrum of N_{31} Nd:glass[32,33] is shown in Fig. 3, where the fluorescence half-line width is 20 nm centered at 1054 nm and normalized to 3.9×10^{-20} cm^2. The gain factor and SECS spectrum of the Nd: glass was fixed after the system was established. Therefore, gain-narrowing compensation via spectral shaping is an efficient way to achieve bandwidth expansion and pulse shape optimization, which can efficiently improve the output capability simultaneously.

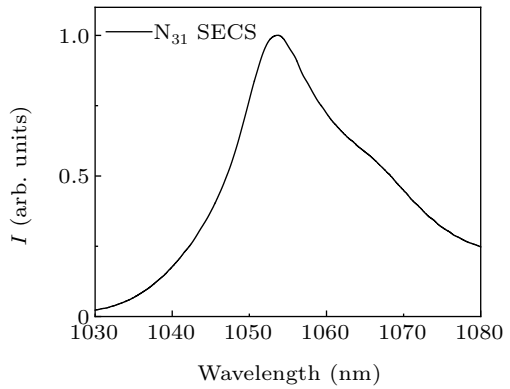


Fig. 3. The normalized SECS spectrum of N_{31} neodymium glass.

In the numerical simulation, an ideal super-Gaussian shape (5th) with a spectral bandwidth of 10 nm (FWHM) and a pulse duration of 5 ns is used as seed, which is fitted from the experimental result of OPCPA. Before the subsequent analysis, the calibration of the simulation to experiment result is done based on the SG PW laser with the gain-narrowing effect. The output spectrum bandwidth of CPA is reduced to 3 nm at 2 kJ with 10 nm and energy of 3 mJ injection, which is shown in Fig. 4(a), and the energy is mainly limited by the B-integral and damage threshold of the mirrors. After that, the goals of energy and spectral bandwidth for CPA amplification are fixed, then the input requirements are obtained by solving the inverse progress of Eqs. (1)–(4).

Figures 4(b)–4(f) show the comparisons of the amplified output spectral bandwidths at goal energy of 2 kJ for 6, 7, 8, 9, and 15 nm (5th Gaussian shape) with gain-narrowing compensation. The spectral shape and energy are simulated at three positions before and after the rod amplifier, and after the disk amplifier in the CPA block.

According to the results in Fig. 4(a), the simulated bandwidth of 10 nm with an injected energy of 3 mJ from OPCPA is reduced to be 3 nm with an output energy of 2 kJ in the SG PW facility, which is consistent with the experimental results. By contrast, figures 4(b)–4(f) display bandwidth expansions for 6, 7, 8, 9, and 15 nm (5th Gaussian shape and 0.5 ns/nm chirped ratio) with the same output energy of 2 kJ, and the required input spectral shape and energy before the rod and disk

amplifier are given at the same time. The detailed parameters of energy, spectral shaping efficiency, and modulation depth defined by the deviation of the intensity between valley and peak at center wavelength are listed in Table 1. The efficiency is evaluated by the ratio of spectrum area (before rod and after disk amplifier for simplifying here). Caused by the SECS of N_{31} neodymium glass (Fig. 3), the highest gain is located at the center wavelength of 1054 nm, which leads to the larger bandwidth expansion needing the deeper modulation at 1054 nm, the wider spectral range, and the larger injected energy.

Table 1. The required input parameters for different bandwidth expansions.

Spectral bandwidth (nm)	3 (no shaping)	6	7	8	9	15
Spectrum range (nm)	1048–1060	1050–1057	1049–1058	1049–1059	1048–1059	1044–1063
Required energy (mJ)	3	4.5	6	12	22	950
Efficiency (%)	100	45	34	26	21	6
Modulation depth (%)		85	93	97	98.6	99.97

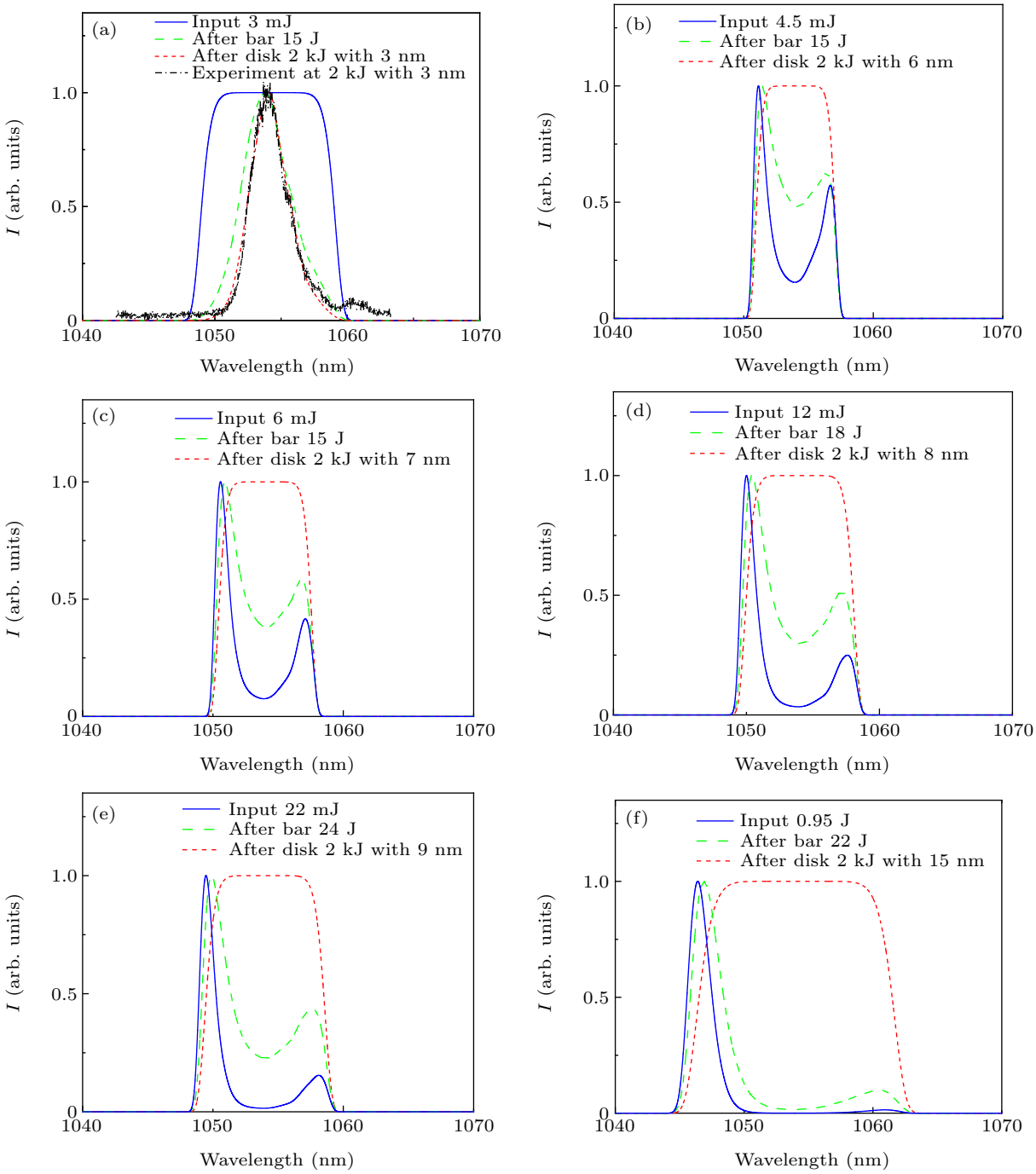


Fig. 4. The required comparisons of spectral shape and energy with output energy of 2 kJ at different positions. (a) Comparison of simulated and experimental results with gain-narrowing. (b)–(f) Bandwidth extended requirements for 6, 7, 8, 9, and 15 nm.

As seen from Fig. 4(a), the output bandwidth after rod amplifier is 3.6 nm, this position no more suits the requirement for bandwidth expansion further, the spectral shaper device should be installed before rod amplifier. On the other hand, considering the nonlinear amplification in OPCPA, the energy stability will get worse when the injected energy and shaped spectrum are changing, and it is more complicated to fix the demand output spectral shape by OPCPA. Therefore, the shaper is set behind the OPCPA in design and experimental demonstration. As shown in Fig. 4(f), in the progress of spectral expansion for 15 nm, the depth of modulation is too deep to be achieved and measured, and the sharper and narrower spectrum brings to higher intensity because of the linear chirp, which makes a larger *B*-integral. After compared, bandwidth expansion of 7 nm is a better choice here, which requires the shaped pulse energy of 6 mJ with an efficiency of 34% as the seed, and the spectral modulation depth is 93% at the center wavelength of 1054 nm.

In addition, to ensure the original function of the SG PW laser, it is demanded to switch quickly between shaping and non-shaping case. Benefit from the thin $LiNbO_3$, which can reduce the effect of beam displacement effectively, need to change nothing except for adding a $LiNbO_3$ birefringent plate in the existing energy adjustable module in OPCPA.

3.2. System *B*-integral and energy output capability for bandwidth expansion

The evaluation of *B*-integral for bandwidth expansion after different amplifiers is given by Fig. 5(a), which is calculated by Eqs. (1)–(4). The system *B*-integral is approximately 1 with bandwidth expansion from 6 nm to 9 nm and increased to the *B*-integral of 1.72 for the bandwidth of 3 nm with gain-narrowing. The simulated parameters are the same as in Fig. 4. However, the *B*-integral for the 15 nm bandwidth expansion is 2.5, which is caused by the significantly spectral modulation in amplification, as displayed in Fig. 4(f). Because of the linear chirp of the broadband pulse, the narrower spectral shape means a shorter pulse duration and results in a higher intensity for bandwidth expansion of 15 nm, which demands higher input energy of 0.95 J. Moreover, the narrower pulse duration goes through more amplifiers until reaching saturation amplification. Those reasons lead to the larger *B*-integral for bandwidth expansion of 15 nm compared to others.

On the other hand, figure 5(b) shows the population inversion of the 350203 amplifier for different bandwidth expansions at 2 kJ. Only 25% of the population in the upper energy level is used, which means that the amplifier can output energy of at least 6 kJ if 75% of the population is employed.

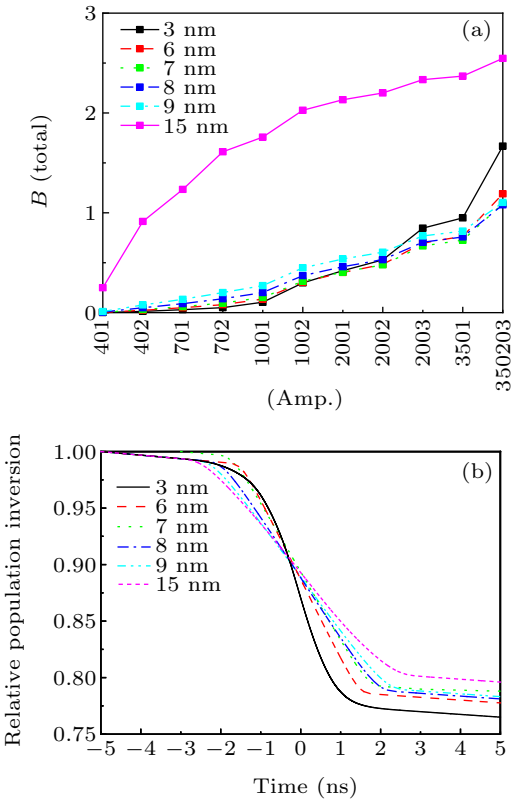


Fig. 5. (a) The cumulative *B*-integral after rod and disk amplifiers; (b) the relative population inversion of 350203 amplifier for different bandwidth expansions of 3, 6, 7, 8, 9, and 15 nm.

3.3. The contrast characteristics with different bandwidth expansions and *B*-integrals

The contrasts with a pulse duration of FTL with a time range of ±10 ps for different bandwidths expansions are compared in Fig. 6, which uses the *B*-integral of Fig. 5(a). As shown in Fig. 6(a), the bandwidth from 3 nm to 9 nm has nearly the same FTL duration of 470 fs, the pulse duration for bandwidth of 15 nm with *B*-integral of 2.5 has not doubled compared to Gaussian shape which *B*-integral above 2[27] and shorter than others, which is benefit from the super-Gaussian shape. The contrasts worsen at −10 ps with bandwidth expansions because of the influence of the spectral shape, which agrees with the results of the gain-narrowing effect.[13] Even so, the contrast can still meet the requirement of $< 10^{-8}$ at −10 ps after bandwidth expansion.

Furthermore, to investigate the energy output capability of the SG PW laser, the influences of the pulse duration and *B*-integral on the contrast with a bandwidth of 7 nm are compared in Fig. 7. Here, the spectrum shape with the bandwidth of 7 nm is checked from Fig. 4(c), and the extra *B*-integral are added to the uncompressed amplified chirped pulse, which is similar to the method.[13] Figure 7(a) shows that the contrasts are 10^{-12}, 10^{-11}, 10^{-9}, and 10^{-8} at −10 ps with *B*-integrals of 1, 2, 3, and 4, while the compressed pulse duration of ∼ 470 fs is given in Fig. 7(b). Because the *B*-integral adds extra frequency chirp to the original linear frequency chirp of the compressed

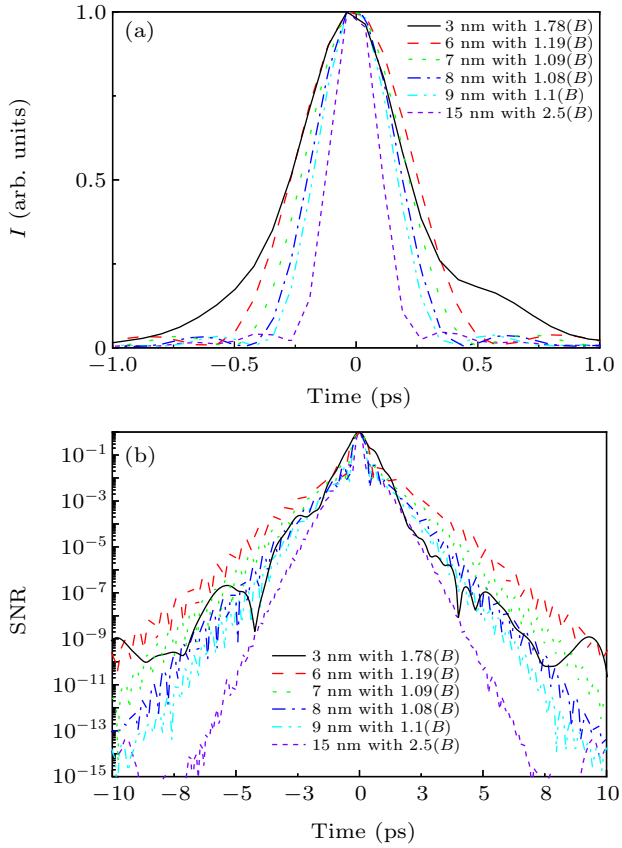


Fig. 6. The pulse durations of FTL (a) and the contrasts (b) with computed *B*-integral (same as Fig. 4) at the time range of ±10 ps for different bandwidths of 3, 6, 7, 8, 9, and 15 nm.

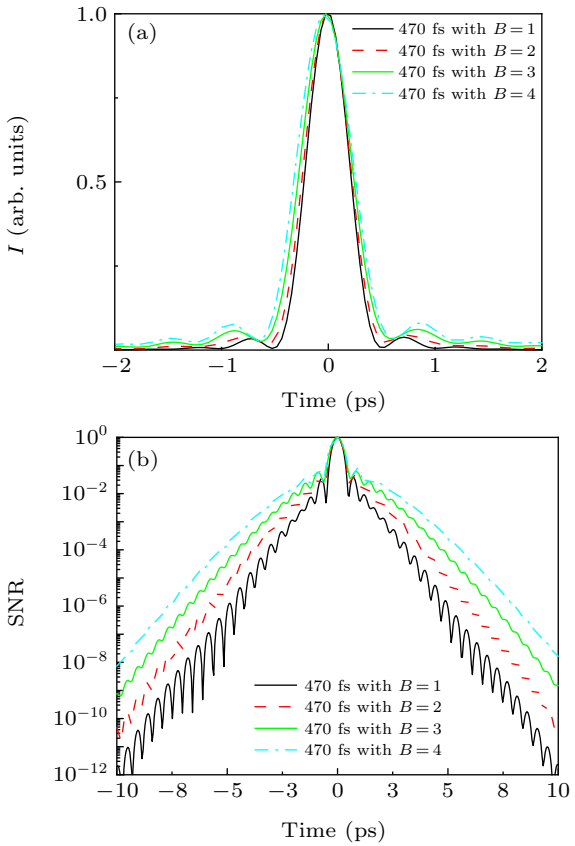


Fig. 7. The compressed pulse is given in linear (a) and log scale (b) for pulse durations of FTL.

pulse and changes the laser power, which makes the contrast smooth but the noise higher as the *B*-integral increases, which are according to similar reported results.[34,35] Compared to the Gaussian spectral shape where *B*-integral should be designed to be ≤ 2, which mainly ensures that the energy is concentrated within twice pulse duration. The cumulative *B*-integral can be designed to π when the spectrum is changed to a super-Gaussian shape similar to the *B*-integral result of 4.5,[17] which can guarantee the contrast of 10^{-8} without pulse duration broadening much. Therefore, compared to the case with gain-narrowing, the energy output capability of the SG PW laser can be effectively increased via bandwidth expansions.

4. Experiment results

To demonstrate the bandwidth expansion effect for the SG PW laser, an experiment was conducted. First, the required parameters for the bandwidth expansion were confirmed. The spectral shape of the OPCPA amplifier is shown in Fig. 8(a), which has a bandwidth of 10 nm centered at 1054 nm with an energy of 60 mJ (RMS = 2%). The output spectrum bandwidth is narrowed to 3 nm FWHM (Fig. 4(a)) with an energy of 2 kJ without spectral shaping. After comparing the required bandwidth, energy, and shaping efficiency, it was concluded that the best choice for bandwidth expansion is 7 nm, which requires the energy of 6 mJ with an efficiency of 34% efficiency and needs 17.6 mJ from the OPCPA with a total energy of 60 mJ.

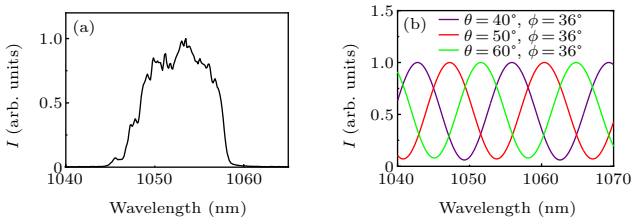


Fig. 8. The output spectrum of OPCPA in the SG PW laser, and the transmission curves of $LiNbO_3$ with $\phi = 36$ degree and $\theta = 40$, 50, and 60 degrees for a 1 mm $LiNbO_3$ birefringent plate.

To compensate the gain-narrowing effect by spectral shaping, and according to Fig. 2, a spectral shaping device was installed behind OPCPA. Based on the OPCPA output spectrum of 10 nm FWHM (Fig. 8(a)), with the goal of bandwidth expansion of 7 nm (Fig. 4(c)), the length of the $LiNbO_3$ birefringent plate is designed and fabricated to be 1 mm with a coating ($T > 98\%$) for 1054 nm ± 20 nm. The designed transmission curves for a 1 mm $LiNbO_3$ are shown in Fig. 8(b), in which the modulated depth of spectrum shaping is achieved by setting the angle of ϕ to 36 degrees, and the center wavelength is controlled by θ to 50 degrees.

The required experimental shaped spectrum is displayed in Fig. 9(a) by adjusting the $LiNbO_3$ birefringent plate, which is measured by optical fiber spectrometer (HR4000 from Ocean). The efficiency of the filter is about 50% and larger than the design of 34% in Table 1, which is caused by the difference of the injected spectrums. The difference between the two is because the spectrum bandwidth of 10 nm from OPCPA is larger than the theoretical design, but the center area of the spectrum is suitable for a bandwidth expansion of 7 nm, and the wavelength range means to have the ability for broadening more with a larger injected energy, as shown in Table 1. The amplified spectrum after CPA is displayed in Fig. 9(b), which is measured by an optical grating spectrometer (ARC-SP-2760 from Princeton Instruments), the detailed modulations come from the noise of the infrared detector. From the compared results, the experimental bandwidth of 7 nm corresponds to the design, and the spectral shaping by the $LiNbO_3$ birefringent plate is effective.

Furthermore, if the energy of the injected shaped seed is increased from 6 mJ to 18 mJ, which can be afforded by nearly updated OPCPA with the energy of 1 J. The output energy after CPA can be increased to be at least 6 kJ with a B-integral less than π, and it can afford 10 PW with a compressed pulse energy of 4.8 kJ (efficiency = 80%) at 480 fs.

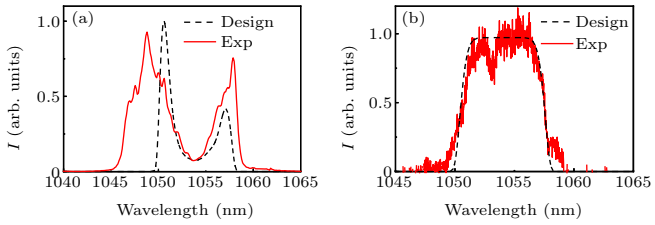


Fig. 9. The results for bandwidth expansion of bandwidth of 7 nm with the energy of 2 kJ, based on the SG PW laser by using $LiNbO_3$ birefringent spectral shaping. The injected (a) and output (b) spectrum of CPA amplification with design (dash line) and experimental (solid line) are demonstrated.

5. Conclusion and perspectives

A bandwidth expansion and pulse shape optimized scheme for the SG PW laser via $LiNbO_3$ birefringent spectral shaping is designed and experimentally demonstrated. The gain-narrowing compensation with different bandwidth expansions is analyzed, and the required injected parameters of the broadband pulse are confirmed. A bandwidth expansion of 7 nm and the energy of 2 kJ with a B-integral of 1 is achieved, which corresponds to the theoretical design. The results indicate that the SG Nd:glass amplifier chain can output energy of more than 6 kJ with a B-integral of π, which can afford the demands of bandwidth and energy for 10 PW laser design with a compressed pulse energy of 4.8 kJ (efficiency = 80%) at 480 fs. The results will be beneficial for the performance improvement of single PW beams and the coherent beam combination of multi-PW beams also in the future.

Acknowledgments

Project supported by the International Partnership Program of Chinese Academy of Sciences (Grant No. 181231KYSB20170022) and the Natural Science Foundation of Jiangsu Higher Education Institutions of China (Grant No. 20KJB140020).

References

[1] Spaeth M L, Manes K R, Kalantar D H, *et al.* 2016 *Fusion Science and Technology* **69** 25
[2] Miquel J L and Prene E 2019 *Nucl. Fusion* **59** 032005
[3] Waxer L J, Maywar D N, Kelly J H, Kessler T J, Kruschwitz B E, Loucks S J, McCrory R L, Meyerhofer D D, Morse S F B, Stoeckl C and Zuegel J D 2005 *Optics and Photonics News* **16** 30
[4] Zhu J Q, Zhu J, Li X C, *et al.* 2018 *High Power Laser Sci. Eng.* **6** e55
[5] Miyanaga N, Azechi H, Tanaka K A, Kanabe T, Jitsuno T, Kawanaka J, Fujimoto Y, Kodama R, Shiraga H, Knodo K, Tsubakimoto K, Habara H, Lu J, Xu G, Morio N, Matsuo S, Miyaji E, Kawakami Y, Izawa Y and Mima K 2006 *J. Phys. IV France* **133** 81
[6] Key M H, Cowan T E, Hammel B A, *et al.* 1998 *17th International Atomic Energy Agency Fusion Energy Conference*, October 19–24, 1998, Yokohama, Japan (to be published)
[7] Stephens R B, Cowan T E, Freeman R R, Hatchett S P, Key M H, Koch J A, Lee R W, MacKinnon A, Pennington D, Snavely R, Tabak M and Yasuike K 2000 *The* 18*th Fusion Energy Conference*, October 4–10, 2000, Sorrento, Italy, IFP-10
[8] Zhang J, Wang W M, Yang X H, Wu D, Ma Y Y, Jiao J L, Zhang Z, Wu F Y, Yuan X H, Li Y T and Zhu J Q 2020 *Phil. Trans. R. Soc. A.* **378** 20200015
[9] Moses E I, Lindl J D, Spaeth M L, Patterson R W, Sawicki R H, Atherton L J, Baisden P A, Lagin L J, Larson D W, MacGowan B J, Miller G H, Rardin D C, Roberts V S, Van Wonterghem B M and Wegner P J 2016 *Fusion Sci. Technol.* **69** 1
[10] Mariscal D, Ma T, Wilks S, *et al.* 2019 *Phys. Plasmas* **26** 043110
[11] Williams G J, Link A, Sherlock M, *et al.* 2020 *Phys. Rev. E* **101** 031201
[12] Hornung J, Zobus Y, Boller P, Brabetz C, Eisenbarth U, Kuhl T, Major Zs, Ohland J B, Zepf M, Zielbauer B and Bagnoud V 2020 *High Power Laser Sci. Eng.* **8** e24
[13] Chuang Y H, Zheng L and Meyerhofer D D 1993 *IEEE J. Q. E.* **29** 270
[14] Kitagawa Y, Fujita H, Kodama R, Yoshida H, Matsuo S, Jitsuno T, Kawasaki T, Kitamura H, Kanabe T, Sakabe S, Shigemori K, Miyanaga N and Izawa Y 2004 *IEEE J. Q. E.* **40** 281
[15] Perry M D, Pennington D, Stuart B C, Tietbohl G, Britten J A, Brown C, Herman S, Golick B, Kartz M, Miller J, Powell H T, Vergino M and Yanovsky V 1999 *Opt. Lett.* **24** 160
[16] Blanchot N, Bignon E, Coic H, *et al.* 2006 *Proc. SPIE* **5975** 59750
[17] Williams W H, Crane J K, Alessi D A, *et al.* 2021 *Appl. Opt.* **60** 2288
[18] Liu L Q, Peng H S, Wei X F, Zhu Q H, Huang X J, Wang X D, Zhou K N, Zeng X M, Wang X, Guo Y, Yuan X D, Peng Z T and Tang X D 2005 *Acta Phys. Sin.* **54** 2764 (in Chinese)
[19] Mansuryan T, Kalashyan M, Lhermite J, *et al.* 2011 *Opt. Lett.* 36 1635
[20] Batysta F, Antipenkov R, Borger T, Kissinger A, Green J T, Kananavičius R, Chériaux G, Hidinger D, Kolenda J, Gaul E, Rus B and Ditmire T 2018 *Opt. Lett.* **43** 3866
[21] Lureau F, Matras G, Chalus O, *et al.* 2020 *High Power Laser Sci. Eng.* **8** e43
[22] Preuss D R and Gole J L 1980 *Appl. Opt.* **19** 702
[23] Heebner J E, Acree R L Jr, Alessi D A, *et al.* 2019 *Appl. Opt.* **58** 8501
[24] Di Nicola J M, Yang S T, Boley C D, *et al.* 2015 *Proc. SPIE* **9345** 934501
[25] Gaul E W, Martinez M, Blakeney J, *et al.* 2010 *Appl. Opt.* **49** 1676
[26] Siders C W, Jovanovic I, Crane J, *et al.* 2006 *International Conference on Ultrahigh Intensity Lasers*, September 25–29, 2006, Cassis, France, UCRL-CONF-222421
[27] Xu G, Wang T, Li Z Y, Dai Y P, Lin Z Q, Gu Y and Zhu J 2008 *Review of Laser Engineering* **36** 1172

[28] Lv B D and Zhang B 1996 *Opt. Commun.* **130** 279
[29] Chu X L, Zhang B, Cai B W, Wei X F, Zhu Q H, Huang X J, Yuan X D, *et al.* 2005 *Acta Phys. Sin.* **54** 4696 (in Chinese)
[30] Zhu X N 1994 *Appl. Opt.* **33** 3502
[31] Zhu S D 1990 *Appl. Opt.* **29** 410
[32] Tang J P, Hu L L, Chen S B, Wang B, Jiang Y S, He D B, Zhang J Z, Li S G, Hu J J and Xu Y C 2011 *Proceeding of International Symposium on Advanced Glass Melting Technology*, May 8–10, 2011, Shanghai, China, p. 87 (in Chinese)
[33] Hu J J, Zhang L Y, Ni J C, Meng T and Hu L L 2020 *Chin. Opt. Lett.* **18** 091402
[34] Perry M D, Patterson F G and Weston J 1990 *Opt. Lett.* **15** 381
[35] Chuang Y H, Meyerhofer D D, Augst S, Chen H, Peatross J and Uchida S 1991 *J. Opt. Soc. Amer. B* **8** 1226